Improved dispersion relations for GaAs and applications to nonlinear optics

T. Skauli,[a] P. S. Kuo, K. L. Vodopyanov, T. J. Pinguet, O. Levi, L. A. Eyres, J. S. Harris, and M. M. Fejer
E. L. Ginzton Laboratory, Stanford University, Stanford, California 94305

B. Gerard, L. Becouarn, and E. Lallier
Thales Research and Technology, F-91404 Orsay, France

(Received 31 March 2003; accepted 2 September 2003)

The refractive index of GaAs has been measured in the wavelength range from 0.97 to 17 μm, which covers nearly the entire transmission range of the material. Linear and quadratic temperature coefficients of the refractive index have been fitted to data measured between room temperature and 95 °C. In the midinfrared, the refractive index and temperature dependence are obtained from analysis of etalon fringes measured by Fourier-transform spectroscopy in undoped GaAs wafers. In the near infrared, the refractive index is deduced from the quasiphasematching (QPM) wavelengths of second-harmonic generation in orientation-patterned GaAs crystals. Two alternative empirical expressions are fitted to the data to give the refractive index as a function of wavelength and temperature. These dispersion relations agree with observed QPM conditions for midinfrared difference-frequency generation and second-harmonic generation. Predictions for various nonlinear optical interactions are presented, including tuning curves for optical parametric oscillators and amplifiers. Also, accurate values are predicted for QPM conditions in which extremely large parametric gain bandwidths can be obtained. © *2003 American Institute of Physics.*
[DOI: 10.1063/1.1621740]

I. INTRODUCTION

GaAs is a material of great technological importance for use in a variety of electronic and electro-optical devices. Thanks to a wide transparency range, between about 0.9 and 17 μm in wavelength, GaAs is also used for infrared optics. In particular, GaAs is seen as a promising material for nonlinear optics[1,2] in the midinfrared due to its favorable material properties, which include high nonlinear susceptibility, low absorption, high laser damage threshold and high thermal conductivity, as well as established material technology. In all optical applications, the refractive index of the material is an essential parameter for device design.

For efficient nonlinear optical interactions, the interacting waves must maintain a constant phase relationship (''phasematching'') throughout the crystal. Birefringent phasematching, which is often used to compensate for dispersion, is not possible in GaAs because it is optically isotropic. However, comparable efficiencies can be obtained by quasiphasematching (QPM), where the nonlinear optical susceptibility of the crystal is periodically modulated (preferably inverted) to compensate for refractive index dispersion.[3] The QPM period for a given set of interacting wavelengths depends critically on the material dispersion. Therefore, design of a QPM structure requires knowledge of the wavelength and temperature dependence of the refractive index with accuracy exceeding that required by most other applications. Conversely, observation of phasematching wavelengths provides a means for accurate characterization of the dispersion.

Initial studies of QPM in GaAs used wafer bonding to fabricate periodic structures.[4] Applications of this technique were limited to long wavelengths ($>4\,\mu$m) and, in most cases, used higher order QPM, which resulted in lower efficiencies for nonlinear interactions.[5,6] More recently, an all-epitaxial process has been developed that permits lithographic definition of the QPM structure. The resulting material is termed orientation-patterned GaAs (OP-GaAs).[7,8] Through a combination of different growth techniques, it has been shown that OP-GaAs can be fabricated with length (20 mm) and thickness (500 μm) sufficient for practical bulk nonlinear interactions. Difference-frequency generation of midinfrared radiation has been demonstrated[2] as has highly efficient second-harmonic generation ($>30\%$ internal efficiency[1]). An important advantage of midinfrared sources based on OP-GaAs is that they can be pumped by well-developed near-IR lasers, thanks to the material's wide transparency range. Important applications of OP-GaAs include spectroscopy, remote sensing and infrared countermeasures.

The refractive index of GaAs has been the subject of numerous publications.[9–17] In addition, the temperature dependence of the refractive index has been treated separately in a number of papers.[18–20] However, many of the previous works considered only part of the spectral transmission window of GaAs. Furthermore, the accuracy provided in earlier literature is not sufficient for QPM applications, especially

[a]Author to whom correspondence should be addressed; also at Norwegian Defense Research Establishment, 2007 Kjeller, Norway; electronic mail: torbjorn.skauli@ffi.no

with short-wavelength pump lasers. These reasons, combined with the renewed interest in GaAs for nonlinear optics, motivate more accurate characterization of the material.

In this article, we present accurate measurements of the dispersion of undoped GaAs and its temperature dependence, based on nonlinear optical measurements as well as on conventional spectroscopic and interferometric techniques. The results are given as physically founded empirical fit functions for the refractive index as a function of wavelength and temperature, which are valid from 0.97 to 17 μm in wavelength (10 350–590 cm^{-1}). This range spans from near the GaAs band gap at 0.87 μm (11 500 cm^{-1}) to the onset of multiphonon absorption.

II. THEORY

A. Quasiphasematching and effect of dispersion errors

Consider a nonlinear interaction between three plane waves of frequencies ω_p, ω_s, and ω_i, termed the pump, signal and idler, respectively, that are related by $\omega_p=\omega_s+\omega_i$. When the waves propagate in a homogeneous, dispersive medium, the phase mismatch between them can be expressed in terms of their wave vectors as $\Delta k=k_p-k_s-k_i$. In a quasi-phase-matched interaction, the phase error that accumulates between waves propagating with different phase velocities is periodically reversed by modulation of the properties of the nonlinear material. The required period of this modulation Λ is given by $2\pi m/\Delta k$, where m, an odd integer,[21] is the QPM order (with $m=1$ being the most efficient case).[3] Λ is given explicitly in terms of vacuum wavelengths and refractive indices as

$$\Lambda=m/(n_p/\lambda_p-n_s/\lambda_s-n_i/\lambda_i). \tag{1}$$

For a given Λ, the acceptance bandwidth of a QPM interaction is dictated by material dispersion and is typically very narrow. To fabricate a QPM structure for a given set of wavelengths, the dispersion must therefore be known very accurately in order to predict Λ.

To estimate the target accuracy for our dispersion relation, consider the case of second-harmonic generation (SHG) with fundamental wavelength λ_ω. In this case, the required QPM period Λ is

$$\Lambda=m\lambda_\omega/(2\Delta n) \tag{2}$$

where $\Delta n=n_{2\omega}-n_\omega$ is the difference in refractive index for fundamental and second-harmonic (SH) waves. Based on Eq. 29 in Ref. 3, we find the error in Δn that leads to a decrease of SHG efficiency by 50% is

$$\delta\Delta n=0.22\lambda_\omega/L, \tag{3}$$

where L is the length of the nonlinear material. For $\lambda_\omega=2\,\mu$m and $L=1$ cm, this refractive index error $\delta\Delta n$ is $\pm 4\times10^{-5}$.

B. Interferometric determination of the refractive index

The refractive index of a plane parallel plate of thickness d can be determined from the etalon interference fringes observable in simple transmission spectroscopy.[11] The roundtrip phase shift of normally incident light in the etalon formed by the plate surfaces is

$$\phi=\frac{4\pi nd}{\lambda}. \tag{4}$$

Ideally, the power transmission T_{plate}, resulting from multiple Fresnel reflections, has the form of an Airy function,

$$T_{\mathrm{plate}}=\frac{1}{1+F\sin^2\phi/2}, \tag{5}$$

where F is given in terms of the Fresnel amplitude reflection coefficient of one interface r as $F=[2r/(1-r^2)]^2$. Even if the shape and amplitude of the fringes are distorted by measurement imperfections, their period and phase depends sensitively on n through Eqs. (4) and (5). At a transmission maximum, the refractive index is given by

$$n(\lambda)=\frac{N\lambda}{2d}, \tag{6}$$

where the integer $N=\phi/2\pi$ is the fringe order, which must be known to determine n. For $d\gg\lambda$, the correct value of N may not be immediately clear from the transmission spectrum if the fringe count is lost towards long wavelengths due to phonon absorption and/or the limited spectral range of the instrument. However, if a physical model of the dispersion at long wavelengths is available, and d is not too large, only one choice of fringe count N for a given peak will make Eq. (6) yield an $n(\lambda)$ consistent with the model over a wide spectral range.[11]

C. Determination of the refractive index using SHG

To supplement interferometric measurements of the refractive index, particularly at shorter wavelengths, we have used QPM SHG interactions of different orders m. From Eq. (2), we see that, at the phasematching wavelength, the refractive index for the second harmonic is given by

$$n(\lambda_\omega/2)=n(\lambda_\omega)+\Delta n=n(\lambda_\omega)+\frac{m\lambda_\omega}{2\Lambda}. \tag{7}$$

In our case, the refractive index at the fundamental wavelength is determined by independent interferometric measurements. Then from SHG measurements, we can use Eq. (7) to determine the refractive index at shorter wavelengths $n(\lambda_\omega/2)$ once we know $n(\lambda_\omega)$.

D. Refractive index temperature dependence

The change in refractive index with temperature can be determined from the temperature dependence of the etalon fringes. For $d\gg\lambda$ and moderate dispersion, the fringe spectrum near a given wavelength is nearly periodic, and temperature-induced changes of this periodicity correspond to changes in the roundtrip phase ϕ. Here we wish to determine temperature variations around room temperature where the refractive index has been accurately measured. A series expansion of ϕ to second order in the deviation ΔT from room temperature gives

$$\phi(\Delta T)\approx\frac{4\pi d}{\lambda}\left[n+\left(n\alpha+\frac{\partial n}{\partial T}\right)\Delta T+\frac{1}{2}\left(2\alpha\frac{\partial n}{\partial T}+n\frac{\partial\alpha}{\partial T}+n\alpha^2+\frac{\partial^2 n}{\partial T^2}\right)\Delta T^2\right], \tag{8}$$

where α is the thermal expansion coefficient of the material, which is well known for GaAs. Given experimentally measured $\phi(\Delta T)$ over a range of temperatures, we fit the coefficients a_0, a_1 and a_2 of a quadratic dependence

$$\phi(\Delta T)\approx a_0+a_1\Delta T+a_2\Delta T^2. \tag{9}$$

By comparing Eq. (9) with Eq. (8), we find

$$\frac{\partial n}{\partial T}=\frac{\lambda}{4\pi d}a_1-n\alpha \tag{10}$$

and

$$\frac{\partial^2 n}{\partial T^2}=\frac{\lambda}{2\pi d}a_2-n\frac{\partial\alpha}{\partial T}-2\alpha\frac{\partial n}{\partial T}, \tag{11}$$

where a numerically small term in α^2 has been neglected.

E. Functional form for the fit expression

To fit the measured dispersion, we use a function of the form given as Eq. (4) by Pikhtin and Yas'kov in Ref. 9:

$$n^2(\hbar\omega)=1+\frac{A}{\pi}\ln\left(\frac{E_1^2-(\hbar\omega)^2}{E_0^2-(\hbar\omega)^2}\right)+\frac{\langle\varepsilon_2\rangle}{\pi}\ln\left(\frac{E_2^2-(\hbar\omega)^2}{E_1^2-(\hbar\omega)^2}\right)+\frac{G_3}{E_3^2-(\hbar\omega)^2}, \tag{12}$$

where $\hbar\omega=hc/\lambda$ is the photon energy (h is the Planck constant and c is the speed of light in vacuum). This form approximates the physical properties of a semiconductor material with band gap E_0. Through Kramers–Kronig relationships, Eq. (12) implies a spectrum for the imaginary permittivity equal to A from E_0 to E_1, $\langle\varepsilon_2\rangle$ from E_1 to E_2, and zero elsewhere apart from an undamped phonon at E_3. This form will hereafter be referred to as the Pikhtin form.

We have also fit a more commonly used Sellmeier-type function with three undamped oscillator terms:

$$n^2(\lambda)=g_0+\frac{g_1}{\lambda_1^{-2}-\lambda^{-2}}+\frac{g_2}{\lambda_2^{-2}-\lambda^{-2}}+\frac{g_3}{\lambda_3^{-2}-\lambda^{-2}}. \tag{13}$$

This expression is also physically based and obeys Kramers–Kronig relationships but, compared to Eq. (12), it represents a more coarse approximation to the material properties.

Temperature dependence of the refractive index is introduced into Eqs. (12) and (13) by adding fitted temperature coefficients to the characteristic energies E_i, wavelengths λ_i, or g_i coefficients.

III. EXPERIMENT

A. Samples

Interferometric measurements were performed using undoped semi-insulating GaAs substrates from Wafer Technology Ltd. with "epitaxy-ready" surface polish on both sides and specified thickness of 500 ± 25 μm. For SHG experiments, we used several OP-GaAs samples grown by a combination of molecular beam epitaxy (MBE) and hydride vapor phase epitaxy (HVPE), described in Ref. 22. The OP-GaAs samples were 500 μm thick and 10 or 20 mm long and had optically polished end facets. The characteristics of the QPM samples are listed in Table I. The QPM periods were defined by photolithography, and the resulting uncertainties in the QPM period are small in comparison to estimates of measurement uncertainty given below.

TABLE I. Characteristics of OP-GaAs QPM samples. The experimentally measured phasematching wavelengths are given for SHG of different QPM orders at $T=21$ °C. The QPM grating period of the sample is shown for $m=1$, and the equivalent first-order QPM period is given for $m>1$.

Sample	Length (mm)	QPM order, m	Equivalent QPM period, Λ/m (μm)	$\lambda_{2\omega}$ (nm)
L	10	1	61.2	2065.9
E	10	1	38.6	1757.5
C	23	1	26.3	1546.8
L	10	3	20.40	1427.3
L	10	5	12.24	1220.3
L	10	9	6.80	1031.4
L	10	11	5.56	979.1
C	23	5	5.26	966.1

B. Transmission spectroscopy measurements

A Perkin-Elmer Spectrum GX Fourier transform infrared (FTIR) spectrometer was used to record transmission spectra through semi-insulating GaAs plates at 22 ± 2 °C from the instrument limit at 1.5 μm in wavelength to the onset of absorption in GaAs at 17 μm. The resolution was 1 cm^{-1}, which was enough to resolve the interference fringes that had periods of about 2.5 cm^{-1}. Due to convergence of the spectrometer beam at the sample focus, residual nonparallelism between the sides of the sample and finite resolution, the observed fringe amplitude was less than that predicted for an ideal plane wave, with significant variations between different samples. For determination of the refractive index at room temperature, we used data from the sample that had the best interference contrast. This sample exhibited $>5\%$ peak-to-peak oscillation in power transmission across the entire spectral range, with increasing amplitude towards longer wavelength.

To characterize the temperature dependence, the sample was placed inside a temperature regulated-aluminum block that was stabilized to within 0.1 °C by a temperature controller. Transmission spectra were recorded at a series of different constant temperatures in approximately 2 °C intervals from 25 to 92 °C. Each step in temperature resulted in a shift of the transmission oscillations by approximately one tenth of a period, as illustrated in Fig. 1. Care was taken to allow time for temperature stabilization before each measurement. The sample temperature was read by a separate thermocouple in contact with the sample. We estimate that this thermocouple measured the actual change in sample temperature

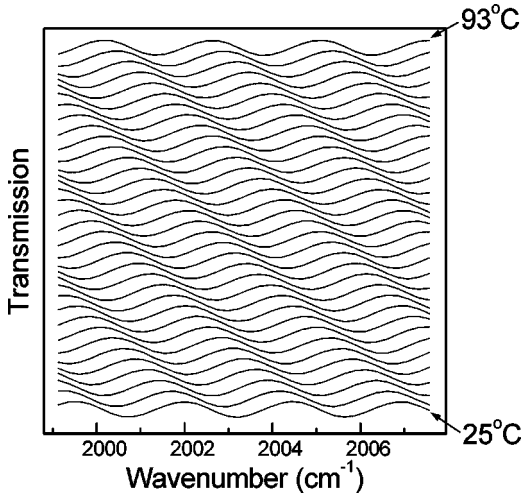

FIG. 1. Example of interference oscillations observed by FTIR transmission spectroscopy at different temperatures. The temperature increment between curves is about 2 °C. For clarity, the curves are offset vertically. The oscillation amplitude here is about 6% peak to peak.

with no more than ± 1 °C error between the lowest and highest temperatures.

C. Laser interferometry

To characterize dn/dT for the shortwave part of the GaAs transmission range not covered by our FTIR spectrometer, we made laser interferometry measurements at 1.064, 1.319, 1.514, 1.550, 1.575 and 2.015 μm. For these measurements, the laser wavelength was held fixed and the sample temperature was ramped 1.0 °C/min from 23 to 95 °C while transmission of the laser beam through the sample was recorded. A typical measurement result is shown in Fig. 2. As above, the temperature of the sample was measured by a separate thermocouple, and the uncertainty was estimated to be less than ± 1 °C between the lowest and highest temperatures.

D. Second-harmonic generation

To determine the refractive index in the spectral range between the short wavelength limit of the FTIR and the GaAs band gap, we exploited the fact that the phasematching wavelengths for nonlinear interactions sensitively depend on dispersion. We used QPM SHG of different orders ($m=1$–11) in several samples to cover a range of second-harmonic wavelengths from 0.97 to 2.07 μm. In this fashion, we were able to obtain the difference of refractive index, $\Delta n = n_{2\omega} - n_{\omega}$, between the fundamental and SH waves using Eq. (7). Table I summarizes the properties of the OP-GaAs samples used and the observed phasematching conditions for SHG of different QPM orders. The SHG data were measured at room temperature, 21 ± 1 °C. A small correction was made to the second-harmonic wavelengths to account for QPM peak shifts that resulted from beam focusing.[23] The corrected values, given in Table I, correspond to a plane-wave interaction for which Eq. (1) holds exactly.

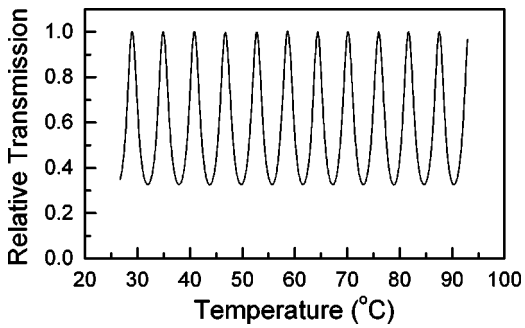

FIG. 2. Sample data showing transmission of a 1575 nm laser beam through a GaAs wafer as a function of the temperature.

In the range of 1.9–3.6 μm, the fundamental beam is produced by an optical parametric oscillator (OPO) based on periodically poled lithium niobate (PPLN). The OPO was pumped by a diode-pumped Nd:YAG laser (Spectra-Physics T-40) with 20 ns pulse width, 1.6 mJ/pulse, repetition rate 100 Hz to 1 kHz. The OPO delivered pulse energies of 100–200 μJ. At longer wavelengths (4–4.2 μm) we used an erbium-laser-pumped, zinc–germanium-phosphide (ZGP) OPO.[24] The focusing conditions of the fundamental beam inside the OP-GaAs crystals were close to confocal. The SHG output was launched into a monochromator (Jobin Yvon Triax 550, 150 grooves/mm grating, calibrated to ± 1 nm with a HeNe laser) or into an optical spectrum analyzer (Advantest Q8384, ± 0.5 nm accuracy) to measure the spectrum of the second harmonic while the fundamental OPO wavelength was tuned.

Measuring the SH while tuning the OPO has the advantage that the broad structure of the OPO spectrum is filtered by the nonlinear interaction. The position and width of the second-harmonic peak are dictated by the QPM condition and are not strongly dependent on the spectral width (or spectral position) of the fundamental beam. This effect was especially important when the PPLN OPO was operated close to degeneracy ($\lambda \approx 2$ μm) where its spectrum became quite broad. The filtering effect is illustrated in Fig. 3, which shows the SH spectrum obtained via fifth-order QPM in OP-GaAs sample C, together with the fundamental OPO spectrum.

In order to validate predictions of the temperature dependence of the SHG phasematching wavelength, OP-GaAs sample L was placed in a temperature regulated aluminum holder and the first-order QPM peak position was measured for several temperatures in the range of 25–150 °C.

E. Difference-frequency generation experiment

For further validation of the model's predictions, difference-frequency generation (DFG) using two near-IR lasers (pump and signal) was performed to generate a midinfrared idler beam. A continuous wave (cw) pump beam (tunable between 1.27 and 1.34 μm at 1–3 mW) was mixed with a 1 W cw signal beam (fixed at 1.536 μm) in an OP-GaAs sample with 26.3 μm QPM period. The resulting idler beam, around 8 μm, was detected by a cooled HgCdTe detector, and the DFG phasematching conditions were measured. The DFG setup is described in detail in Ref. 2. The quasiphase-matching wavelengths were determined for several

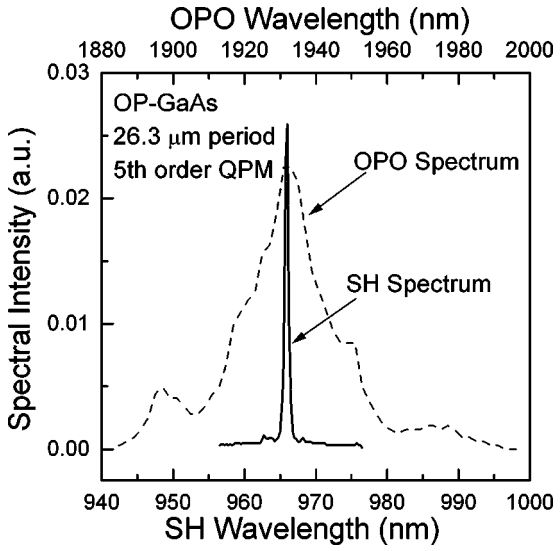

FIG. 3. Second-harmonic (SH) spectrum obtained via fifth-order QPM in OP-GaAs, with grating period 26.3 μm and length 10 mm, shown together with the fundamental OPO spectrum. The SH spectrum is sharply defined due to the narrow width of the QPM peak.

GaAs sample temperatures between 30 and 110 °C. QPM peak shifts due to focusing are negligible for the DFG experiment, and no correction for this effect was made.

IV. DATA ANALYSIS AND RESULTS

A. Refractive index at room temperature

The refractive index down to 1.5 μm can be calculated from the FTIR transmission fringe maxima using Eq. (6), provided that fringe order N and sample thickness d can be determined. In the following, we show that only one choice of fringe order and a very narrow range of thickness are consistent with the combined FTIR and SHG data.

We first determined the position of all transmission fringe maxima in the FTIR spectrum (by local least-squares fitting of a sine to the transmission spectrum over successive overlapping spectral intervals a few fringes wide). The absolute fringe order N at the long wave end of the measured FTIR spectrum could be uniquely determined by trying different values[11] and fitting the Pikhtin (or Sellmeier) expression to the resulting refractive index values. If an incorrect fringe count is used, the resulting refractive index values diverge towards long wavelengths, and the shape of the dispersion becomes highly inconsistent with physical models of the dispersion.

Dotted lines in Fig. 7 illustrate the effect of offsetting all fringe orders by ± 1 relative to our best fit. Even if the Pikhtin or Sellmeier expressions are refitted to data with incorrectly chosen fringe orders, the resulting fit function invariably exhibits large systematic deviations from the data. In the case of a ± 1 offset in fringe order, the average deviation of the best fit to the resulting data is more than 10 times larger than that for the fit obtained using the correct fringe order.

The thickness d then remains to be determined, but cannot readily be measured mechanically to within the same accuracy as the fit of FTIR fringe peak positions. A simple

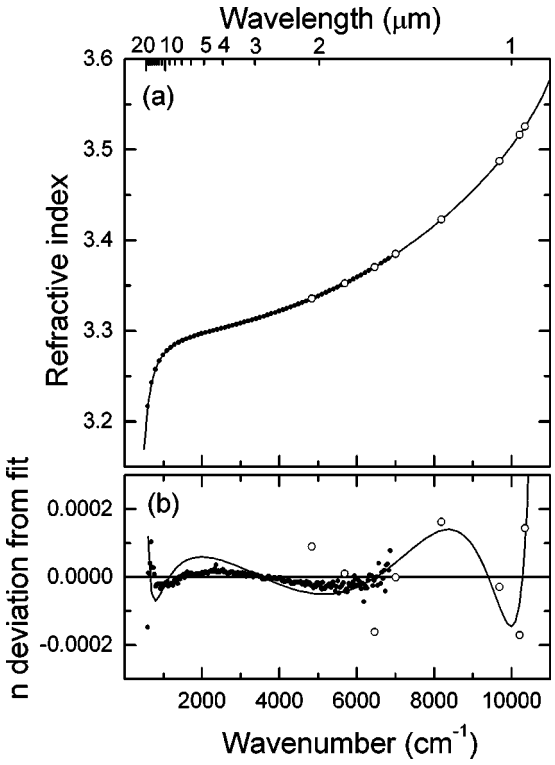

FIG. 4. (a) GaAs refractive index at 22 °C obtained from FTIR spectroscopy and from QPM SHG experiments. The solid line is calculated from Eq. (12) using the parameters listed in Table II. (b) Refractive index deviations from the Pikhtin form fit, Eq. (12). The solid line shows the deviation of the fitted Sellmeier form, Eq. (13), from the Pikhtin fit. For both plots, closed and open circles indicate FTIR and SHG data, respectively. Every 10th point is shown in (a) for clarity.

mechanical measurement of the sample gave a thickness of 516 μm, with an estimated uncertainty of $\pm 3\,\mu$m or $\pm 0.6\%$.

The thickness can be determined somewhat more accurately than by mechanical measurement by combining FTIR and SHG data. Note that the SHG measurements give the difference in refractive index Δn according to Eq. (2) without reference to d, relying only on the QPM period which is accurately determined by photolithography. In contrast, Δn from the FTIR measurement varies inversely with d, as is implied by Eq. (6). For the first three SHG data points, both the fundamental and second harmonic are within the FTIR spectral range. The sample thickness d can be estimated by requiring consistency between Δn values obtained from FTIR and SHG.

For these data points, we find that the mean difference between Δn_{FTIR} and Δn from SHG is zero if we assume a thickness of 514.1 μm, with standard deviation of the mean equivalent to a $\pm 0.2\%$ variation in thickness. The relative uncertainties in wavelength and fringe count are small compared to this uncertainty in thickness. Therefore we estimate the uncertainty of n to be 0.2%.

Thus without reference to other measurements, the combined FTIR and SHG data provide a unique determination of fringe order and an accurate measurement of thickness. Together, these data result in the set of measured refractive index values that are plotted in Fig. 4.

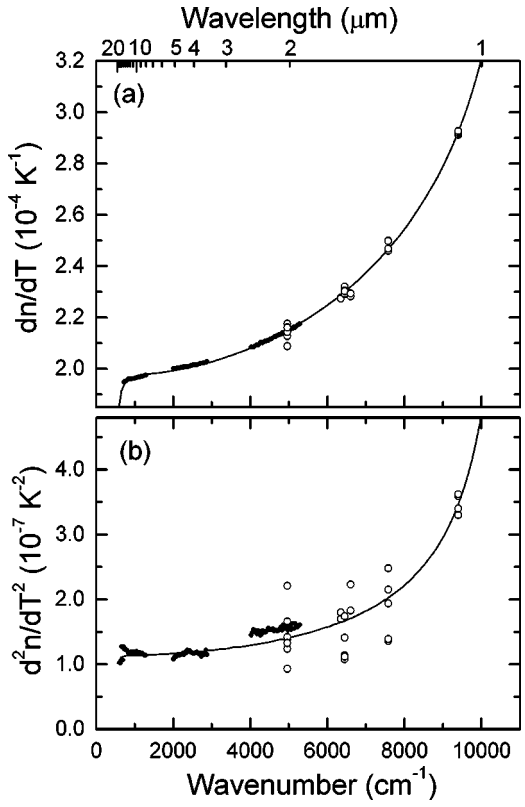

FIG. 5. GaAs refractive index temperature dependence: (a) dn/dT and (b) d^2n/dT^2 at 22 °C, determined by FTIR (closed circles) and laser interferometry (open circles). The solid line is calculated from the fitted model. In both (a) and (b), the Pikhtin and Sellmeier fits are indistinguishable from each other.

B. Temperature dependence of the refractive index

To obtain the temperature dependence from FTIR transmission data recorded at different temperatures, we first determined the temperature-induced phase shift of the interference oscillations (from the phase shift of a locally fitted sine as a function of the temperature). This phase shift is identical to a shift in ϕ given by Eq. (8). The coefficients of Eq. (9) were determined from these data by least-squares fits. The resulting coefficients were extensively scattered in a few spectral regions with low oscillation amplitude because of slight nonparallelism in the faces of the sample used for measurement of the temperature dependence. These regions were excluded from the subsequent analysis.

For the laser transmission data recorded at shorter wavelengths, the transmission measured as a function of the temperature was fit directly to a combination of Eqs. (5) and (9). The fit parameters were F, a_0, a_1 and a_2.

The combined FTIR and laser transmission measurements gave linear and quadratic temperature coefficients for ϕ over the wavelength range from 1.064 to 17 μm. From these temperature coefficients, we determined dn/dT and d^2n/dT^2 using Eqs. (10) and (11). We have assumed $\alpha = 5.756\times10^{-6}$ K^{-1} and $d\alpha/dT = 5.5\times10^{-9}$ K^{-2} at room temperature for GaAs.[25] The resulting temperature dependence of the refractive index is shown in Fig. 5.

We estimate that the uncertainty in the measured linear temperature dependence is dominated by the ±1 °C temperature uncertainty in the 70 °C interval of the experiment. This contributes a relative uncertainty of $\pm1.4\%$ in dn/dT. For the second-order temperature dependence, the data exhibit scatter of about $\pm15\%$.

TABLE II. Fitted parameters for the temperature dependent dispersion given by Eqs. (12) and (13). ΔT is the deviation from the reference temperature 22 °C. For Eq. (12), the photon energy in eV was calculated as $\hbar\omega = 1.239\,842/\lambda$ with λ given in μm.

Parameter	Value
Pikhtin form, Eq. (12)	
E_0 (eV)	$1.425\,000 - 0.000\,371\,64\,\Delta T - 7.497\times10^{-7}\,\Delta T^2$
E_1 (eV)	$2.400\,356 - 0.000\,514\,58\,\Delta T$
E_2 (eV)	$7.691\,979 - 0.000\,465\,45\,\Delta T$
E_3 (eV)	$0.034\,303 + 0.000\,011\,36\,\Delta T$
$\langle\varepsilon_2\rangle$	12.993 86
G_3	0.002 181 76
A	0.689 578
Sellmeier form, Eq. (13)	
λ_1 (μm)	$0.443\,1307 + 0.000\,050\,564\,\Delta T$
λ_2 (μm)	$0.874\,6453 + 0.000\,1913\,\Delta T - 4.882\times10^{-7}\,\Delta T^2$
λ_3 (μm)	$36.9166 - 0.011\,622\,\Delta T$
g_0	5.372 514
g_1	27.839 72
g_2	$0.031\,764 + 4.350\times10^{-5}\,\Delta T + 4.664\times10^{-7}\,\Delta T^2$
g_3	0.001 4363 6

C. Empirical fit function

Pikhtin and Yas'kov's dispersion expression, Eq. (12), and the Sellmeier form, Eq. (13), are fitted to the room temperature data in Fig. 4(a). FTIR and SHG data were weighted differently in the fits to account for different sampling densities. The resulting fit parameters are given in Table II.

Both forms provide an excellent fit to the measured data, as seen in Fig. 4. In the Pikhtin form, the parameter E_0 is fixed to 1.425 000 eV, a number close to the literature value for the band gap at 295 K.[26] Allowing E_0 to vary along with all the other parameters (listed in Table II) caused E_0, E_1 and E_2 to move far away from their corresponding physical energies,[9] at which point the dispersion model is no longer based on true critical energies and is thus highly unphysical. For the Sellmeier form, all parameters are varied. The difference between the fits is comparable to the scatter in the data, and the amount of scatter is very similar for the two fits.

The effect of the temperature is empirically modeled by adding linear and quadratic temperature coefficients to the characteristic energies E_i of the fitted Pikhtin form and wavelengths λ_i and g_i coefficients of the fitted Sellmeier form. The quadratic temperature coefficients were added to the parameters associated with the band gap (E_0 for the Pikhtin form, λ_2 and g_2 for the Sellmeier form). No statistically significant improvement to the fit was obtained by allowing additional energy terms to have quadratic temperature dependence. The linear-coefficient values are determined by fitting the temperature derivatives of the dispersion expressions to the dn/dT data in Fig. 5(a). The qua-

dratic temperature coefficients of the fit are found from the fit to the d^2n/dT^2 data, as shown in Fig 5(b).

D. Comparison of fit functions with QPM results

Comparison with observed QPM peak wavelengths represents a sensitive test of the fitted dispersion relation. Since the fit is partly based on QPM SHG, good agreement with these experiments is expected. Figure 4 illustrates agreement with the SHG data over more than an octave including the region near the band gap. The scatter in the SHG refractive index data around the fits, shown in Fig. 4(b), is probably due to a combination of errors in the determination of the second-harmonic wavelength and variations in sample temperature. We find that residual scatter around the fitted function is comparable to that expected from the experimental uncertainties, with the Pikhtin form performing slightly better, on average.

As a further test, the fitted temperature-dependent refractive index expressions can be compared to the observed temperature dependence of the SHG and DFG experiments shown in Fig. 6. Near room temperature, the observed tuning rate of the SHG phasematching wavelength at 4 μm fundamental is predicted to within 5% by both the Pikhtin and Sellmeier fits. The Pikhtin fit coincides with the data, within the intervals of uncertainty, while the Sellmeier fit exhibits some excess offset, equivalent to a 10 °C error in temperature. This offset is easily compensated for in practical OP-GaAs applications. For the DFG experiment, both fits coincide with the data within the intervals of uncertainty. The observed DFG tuning rate near room temperature is predicted to within 5% by the Pikhtin fit and to within 3% by the Sellmeier fit.

We also compared our predictions with experimental data for longwave difference-frequency generation in diffusion-bonded-stacked (DBS) GaAs, described in Ref. 6. The experiment measured a peak wavelength of 16.6 μm generated by third-order QPM in a DBS GaAs sample with 252 μm average plate thickness. Our dispersion relation predicted a peak wavelength of 16.5 μm. The small deviation in wavelength can be explained by an uncertainty of ± 1 μm in the plate thickness.

In addition, we found that our predictions are in excellent agreement with the experimental results that measured DFG coherence lengths in bulk GaAs in the wavelength range 8–12 μm reported in Ref. 27.

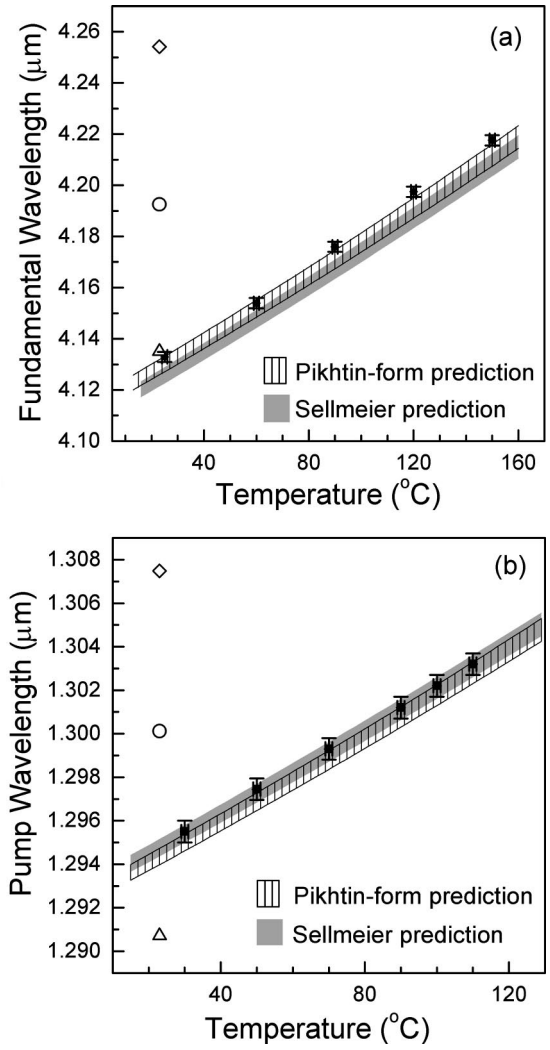

FIG. 6. Comparison of predicted and measured phasematching wavelengths. Closed squares are measured quasiphasematching wavelengths at different temperatures. The shaded bands give the QPM wavelengths predicted by the fitted Pikhtin (striped) and Sellmeier (gray) functions and reflect the uncertainty in the dispersion models. Open symbols represent room temperature predictions of Ref. 11 (diamonds) and of Eqs. (3) (circles) and (4) (triangles) in Ref. 9. (a) Fundamental wavelength for second-harmonic generation in a sample with QPM period of 61.2 μm. (b) Pump wavelength for difference frequency generation with the signal wavelength fixed at 1.536 μm in a sample with QPM period of 26.3 μm.

V. DISCUSSION

A. Uncertainty of the fitted expressions

The random scatter of the data is exceeded by the $\pm 0.2\%$ systematic uncertainty arising from the thickness determination, so this latter value can be taken as the uncertainty in our fitted dispersion functions. From Eq. (6), we see that the uncertainty in d leads to errors that are highly correlated since the resulting n at different wavelengths will be scaled by the same value of d.

Furthermore, Eq. (6) also implies that the relative uncertainty in index difference Δn is the same as the relative uncertainty in d, that is, $\pm 0.2\%$, since the $N\lambda$ products are very accurately known. The accuracy of predicted QPM wavelengths depends on the accuracy of Δn values obtained from the fitted expression. As an extreme example, consider the case of frequency doubling 2 μm radiation. For this case, $\Delta n \approx 0.17$ with uncertainty of $\pm 3\times 10^{-4}$. Note that if one were to perform independent measurements of $n(\lambda)$ and $n(\lambda/2)$, the individual refractive indices would need to be measured to at least $0.2\% \times \Delta n/(\sqrt{2}n) \approx 0.007\%$ accuracy to reproduce the QPM prediction accuracy of our measurements.

The uncertainty in Δn of $\pm 3\times 10^{-4}$ is still a factor of 8 larger than the target accuracy of $\pm 4\times 10^{-5}$ estimated from Eq. (3) for the stringent case of doubling 2 μm radiation. However, this uncertainty in Δn can be compensated by about 3 °C of temperature tuning or 1.3 nm of wavelength

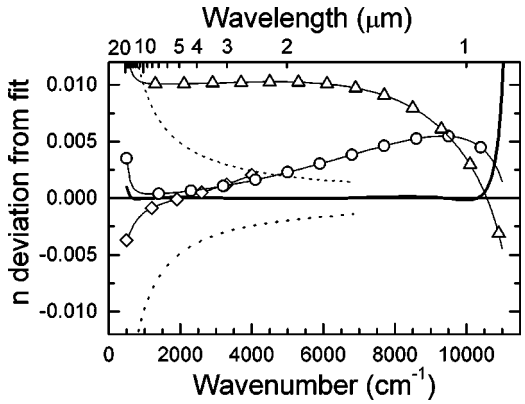

FIG. 7. Shown are deviations from our fitted Pikhtin form, Eq. (12), for Ref. 11 (diamonds) and for Eqs. (3) (circles) and (4) (triangles) of Ref. 9. Also shown is deviation of the fitted Sellmeier form presented here (solid line). Beyond the range of data from 0.97 to 17 μm, extrapolation of our fits is likely to yield increasingly inaccurate values. Dotted lines show the amount of change in experimental refractive index values resulting from errors of ± 1 in the assumed fringe order N.

tuning. The accuracy of our fit functions appears to be sufficient for practical applications.

For first-order and second-order temperature dependence, we estimate fit uncertainties of $\pm 1.4\%$ and $\pm 15\%$, respectively. We note that because the quadratic temperature dependence is very weak, the error from d^2n/dT^2 becomes comparable to the error in dn/dT only when taken over a 100 °C temperature range. Furthermore, over the range of temperatures measured (22–95 °C), the uncertainty in the refractive index at a given wavelength is dominated by the 0.2% uncertainty from the dispersion fit itself and not from errors in the temperature derivatives. It is also important to note that the uncertainties in n are correlated whereas the uncertainties in dn/dT and d^2n/dT^2 are not correlated. This observation has implications for QPM where differences in n are important. Because the uncertainties in Δn at room temperature are small, the uncertainties for QPM predictions at moderate temperatures may be dominated by uncertainties from the temperature derivatives.

B. Comparison with previously published results

Pikhtin and Yas'kov[9] quoted an experimental uncertainty of 0.003 for n. Moore and Holm[11] scaled their refractive index to coincide with Eq. (3) of Pikhtin and Yas'kov around 2 μm wavelength, and estimated additional uncertainty of 0.2%. Figure 7 shows that their work is in agreement with our data within the respective uncertainties.

However, Fig. 6 illustrates that the fit functions given here predict QPM wavelengths at room temperature with accuracy significantly better than previous fits. Figure 6 shows that the large deviations of predictions using previous dispersion functions are not easily compensated by temperature tuning. The QPM wavelength predictions based on dispersion functions presented in this article are much closer to observations. The correlated scaling error that dominates our measurements has a relatively small effect on predicting phasematching conditions compared to the uncertainties in other dispersion relations.

Della Corte *et al.*[19] have made extensive measurements of the GaAs refractive index temperature dependence at 1.5 μm. They found $dn/dT = 2.34\times10^{-4}$ K^{-1} at room temperature, which is very close to the value of 2.33×10^{-4} K^{-1} obtained from our fits. For d^2n/dT^2 we find a value of 1.7×10^{-7} K^{-2} at 1.5 μm. The results of Della Corte *et al.* imply a value of 2.4×10^{-7} K^{-2} with no estimate of uncertainty given.

C. Discussion and comparison of our fits

The Sellmeier expression implies an absorption spectrum consisting of narrow lines, which clearly is a poor description of GaAs optical properties above the band gap energy. The Pikhtin expression, on the other hand, is closer to the physical situation. The authors of Ref. 9 take literature values for the critical energies E_0, E_1, E_2 and E_3, derive expressions for A and G_3 and determine a value for $\langle\varepsilon_2\rangle$ by fitting to measured data. The resulting model agrees well with measurements. As shown here, the fit to our data can be significantly improved by allowing more parameters to be varied. As a result, however, our fitted parameters cannot be considered to have a quantitative physical significance because of the coarse approximation to the shape of the absorption spectrum implied by Eq. (6).

We note that when the two fitted expressions are used to extrapolate the refractive index towards the band gap, they both deviate from the shape of the data tabulated in Ref. 10 for dispersion near the band gap. These data instead follow closely the curve of Eq. (3) in Ref. 9. Thus using the fits presented here to extrapolate towards shorter wavelengths must be done with caution, particularly in the case of the Sellmeier fit, which diverges rapidly from the shape of the dispersion measured near the band gap.

Given a free choice between the two fit functions, we recommend the Pikhtin form, Eq. (12), because of its slightly better overall agreement with measurements and the closer approximation to the material physics. However, the Sellmeier form, Eq. (13), is more commonly used and may be more convenient for use in existing software tools.

D. Some implications of the results for QPM

Figure 8 shows possible phasematching conditions for a selected set of pump wavelengths. Figure 8 also shows the effect of changing the temperature by 100 °C. The plot illustrates that, in some cases, a substantial amount of temperature tuning is possible. Figure 8 also indicates that for pump wavelengths in the vicinity of 3 μm, where the tuning curve becomes nearly vertical, large bandwidths can be obtained. Figure 9 shows examples of predicted parametric gain spectra in this region. Depending on the gain flatness requirement, bandwidths up to about 1.5 octaves are obtained. Wide bandwidths can be obtained for pump wavelengths in the range from about 3.06 to 3.22 μm.

VI. CONCLUSIONS

We have measured the refractive index of GaAs, as well as its temperature dependence, in the spectral region of the crystal's optical transparency, from 0.97 to 17 μm, and in the

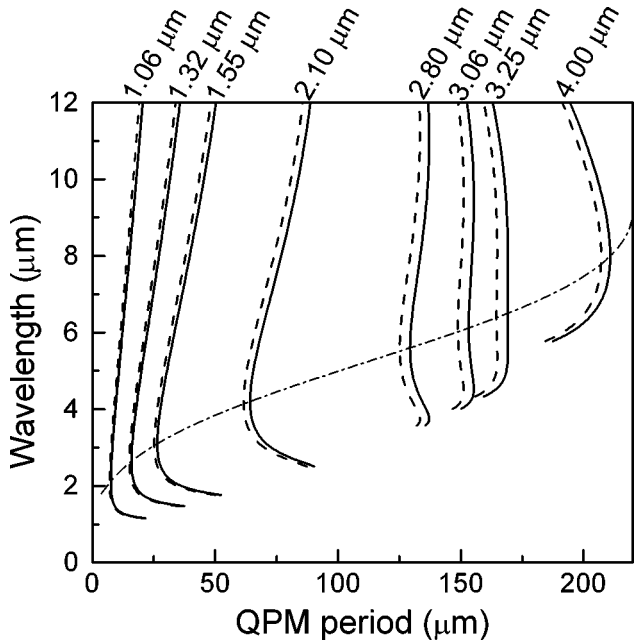

FIG. 8. Predicted phasematched signal and idler pairs as a function of the QPM period for the pump wavelengths indicated at the top. The solid and dashed lines are for 20 and 120 °C, respectively. The dash-dotted line indicates degeneracy at room temperature. No significant difference between the two fits is seen on this scale.

range of temperatures between 22 and 95 °C. To derive the refractive index, we have used several interferometric techniques, as well as QPM nonlinear optical frequency conversion of different QPM orders (1st–11th order) in orientation-patterned GaAs. Two expressions for the refractive index as a function of wavelength and temperature were fitted to measured data. The estimated uncertainty of the refractive index data and the fitted functions is 0.2%, which is dominated by a systematic scaling error, rather than random scatter. Refractive index differences between different wavelengths can be predicted within the same uncer-tainty of 0.2%, which corresponds to uncorrelated errors of no more than

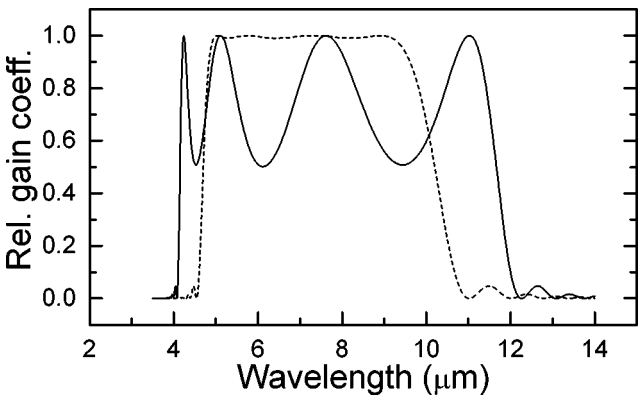

FIG. 9. Parametric gain coefficient for QPM interactions scaled to the peak value in 10 mm long GaAs gratings where the period Λ has been optimized for large bandwidth. The solid line represents a pump wavelength of 3.059 μm, which results in a bandwidth of 4.1–11.7 μm with relative gain variations of 50%. The dashed line represents a pump wavelength of 3.217 μm, which results in less than 1% variation in gain from 4.9 to 9.2 μm. The values shown are calculated using the fitted Pikhtin form at 20 °C.

$\pm 0.007\%$ in the refractive index at the wavelengths involved. Both fitted dispersion relations are in excellent agreement with numerous QPM nonlinear optical experiments. The agreement is superior to that given by previous dispersion relations found in the literature. Residual prediction errors can typically be compensated by small (less than 5 °C) temperature adjustments. Our results enable accurate design of QPM structures based on GaAs, such as temperature tunable devices or optical amplifiers with extremely wide parametric gain bandwidths.

ACKNOWLEDGMENTS

This research was sponsored in part by the Air Force Office of Scientific Research (AFOSR) under AFOSR Grant Nos. F49620-01-1-0428 and F49620-99-1-0270 and by Sandia National Laboratories Contract No. 4489 (under a Department of Energy prime contract). This material was also based upon work supported in part by the U.S. Army Research Office (ARO) under ARO Grant No. DAAAH04-96-1-0002. The authors acknowledge the support of Picarro, Inc. for the use of the PPLN and ZGP OPOs and FTIR spectrometer. One of the authors (P.S.K.) acknowledges support by the Lucent Graduate Research Program for Women.

[1] T. Skauli *et al.*, Opt. Lett. **27**, 628 (2002).
[2] O. Levi *et al.*, Opt. Lett. **27**, 2091 (2002).
[3] M. Fejer, G. A. Magel, D. H. Jundt, and R. L. Byer, IEEE J. Quantum Electron. **28**, 2631 (1992).
[4] L. A. Gordon, R. C. Eckardt, and R. L. Byer, Proc. SPIE **2145**, 316 (1994).
[5] E. Lallier, M. Brevignon, and J. Lehoux, Opt. Lett. **23**, 1511 (1998).
[6] D. Zheng, L. A. Gordon, Y. S. Wu, R. S. Feigelson, M. M. Fejer, R. L. Byer, and K. L. Vodopyanov, Opt. Lett. **23**, 1010 (1998).
[7] C. B. Ebert, L. A. Eyres, M. M. Fejer, and J. S. Harris, J. Cryst. Growth **201**, 187 (1999).
[8] S. Koh, T. Kondo, Y. Shiraki, and R. Ito, J. Cryst. Growth **227**, 183 (2001).
[9] A. N. Pikhtin and A. D. Yas'kov, Sov. Phys. Semicond. **12**, 622 (1978).
[10] E. D. Palik, *Handbook of Optical Constants of Solids* (Academic Press, Orlando, FL, 1985).
[11] W. J. Moore and R. T. Holm, J. Appl. Phys. **80**, 6939 (1996); **81**, 3732 (1997).
[12] C. Palmer, P. N. Stavrinou, M. Whitehead, and C. C. Phillips, Semicond. Sci. Technol. **17**, 1189 (2002).
[13] D. T. F. Marple, J. Appl. Phys. **35**, 1241 (1964).
[14] S. Gehrsitz, F. K. Reinhart, C. Gourgon, N. Herres, A. Vonlanthen, and H. Sigg, J. Appl. Phys. **87**, 7825 (2000).
[15] C. Tanguy, IEEE J. Quantum Electron. **32**, 1746 (1996).
[16] S. Adachi, J. Appl. Phys. **53**, 5863 (1982).
[17] S. Adachi, J. Appl. Phys. **58**, R1 (1985).
[18] M. Bertolotti, V. Bogdanov, A. Ferrari, A. Jascow, N. Nazorova, A. Pikhtin, and L. Schirone, J. Opt. Soc. Am. B **7**, 918 (1990).
[19] F. G. Della Corte, G. Cocorullo, M. Iodice, and I. Rendina, Appl. Phys. Lett. **77**, 1614 (2000).
[20] C. Tanguy, J. Appl. Phys. **80**, 4626 (1996).
[21] Even m is permitted when the modulation duty cycle deviates from the optimal 50% (after Ref. 3).
[22] L. A. Eyres, P. J. Tourreau, T. J. Pinguet, C. B. Ebert, J. S. Harris, M. M. Fejer, L. Becouarn, B. Gerard, and E. Lallier, Appl. Phys. Lett. **79**, 904 (2001).
[23] G. D. Boyd and D. A. Kleinman, J. Appl. Phys. **39**, 3597 (1968).
[24] K. L. Vodopyanov, F. Ganikhanov, J. P. Maffetone, I. Zwieback, and W. Ruderman, Opt. Lett. **25**, 841 (2000).
[25] R. R. Reeber and K. Wang, Mater. Res. Soc. Symp. Proc. **622**, T6.35.1 (2000).
[26] J. S. Blakemore, J. Appl. Phys. **53**, R123 (1982).
[27] R. Haidar, A. Mustelier, Ph. Kupecek, E. Rosencher, R. Triboulet, Ph. Lemasson, and G. Mennerat, J. Appl. Phys. **91**, 2550 (2002).